7.10 THE MODIFIED COMPRESSION FIELD THEORY

Figure 7-34 illustrates the stress field in the web of a non-prestressed beam before and after cracking. Prior to cracking, the shear is carried equally by diagonal tensile and diagonal compressive stresses acting at 45°. After diagonal cracks form the tensile stresses in the concrete are substantially reduced. In the compression field theory it is assumed that the principal tensile stress, f_1, equals zero after the concrete has cracked. On the other hand, the modified compression field theory accounts for the contribution of the tensile stresses in the concrete between the cracks (see Fig. 7-34c).

The equilibrium conditions for the modified compression field theory will be introduced using the symmetrical cross section subjected to pure shear shown in Fig. 7-35. The total area of longitudinal prestressing tendons in the section is A_{px} and the total area of non-prestressed reinforcement is A_{sx}. The shear on this section will be resisted by the diagonal compressive stresses, f_2, together with the diagonal tensile stresses, f_1. It should

Figure 7-32 Reinforced concrete element failing in shear. From Vecchio and Collins (Ref. 7-35).

be recognized that the tensile stresses in the diagonally cracked concrete vary in magnitude from zero at the crack locations to peak values between the cracks (see Fig. 7-35b). As the equilibrium equations are obtained by integrating the stresses over the cross section it is appropriate to use the average value of the tensile stresses when formulating these equilibrium expressions.

From the Mohr's stress circle shown in Fig. 7-35c, the following relationship for the principal compressive stress, f_2, can be derived:

$$f_2 = (\tan\theta + \cot\theta)\, v - f_1 \tag{7-27}$$

where

$$v = \frac{V}{b_w jd} \tag{7-5}$$

The diagonal compressive stresses push apart the flanges of the beam while the diagonal tensile stresses pull them together (see Fig. 7-35). The unbalanced component must be carried by tension in the web reinforcement. This equilibrium requirement can be expressed as

$$A_v f_v = (f_2 \sin^2\theta - f_1 \cos^2\theta) b_w s$$

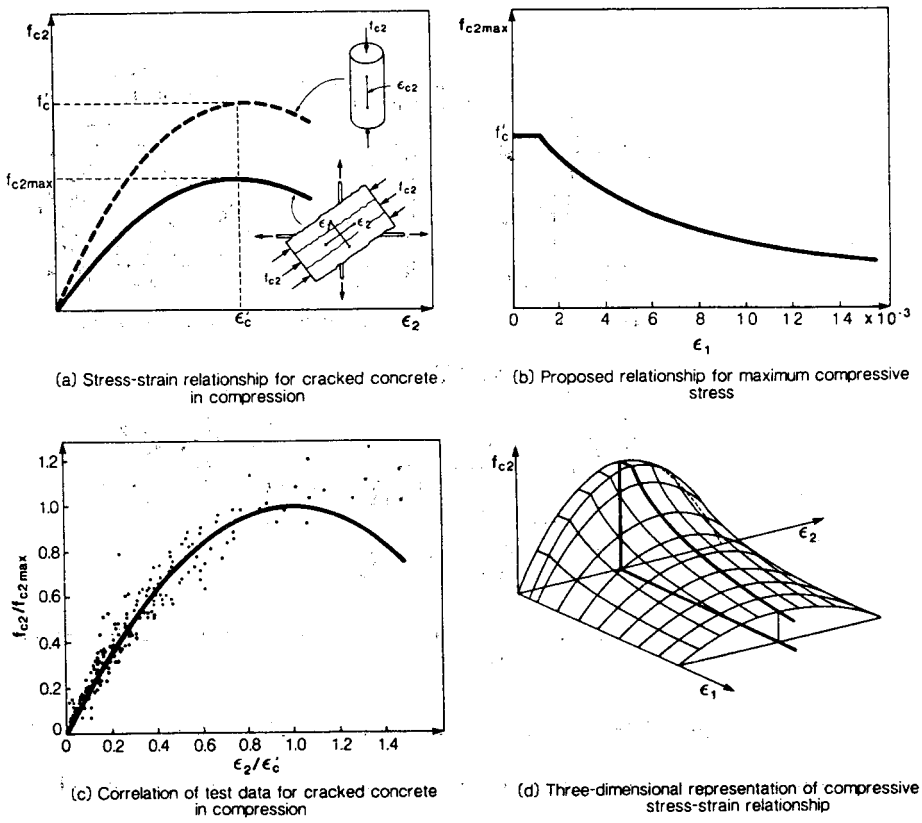

(a) Stress-strain relationship for cracked concrete in compression

(b) Proposed relationship for maximum compressive stress

(c) Correlation of test data for cracked concrete in compression

(d) Three-dimensional representation of compressive stress-strain relationship

Figure 7-33 Compressive stress-strain relationship for cracked concrete.

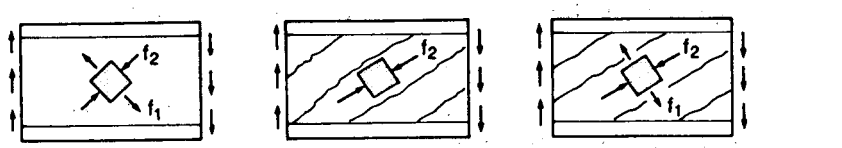

(a) Before cracking $f_1 = f_2$, $\theta = 45°$

(b) Compression field theory, $f_1 = 0$

(c) Modified compression field theory, $f_1 \neq 0$

Figure 7-34 Stress fields in web of reinforced concrete beam.

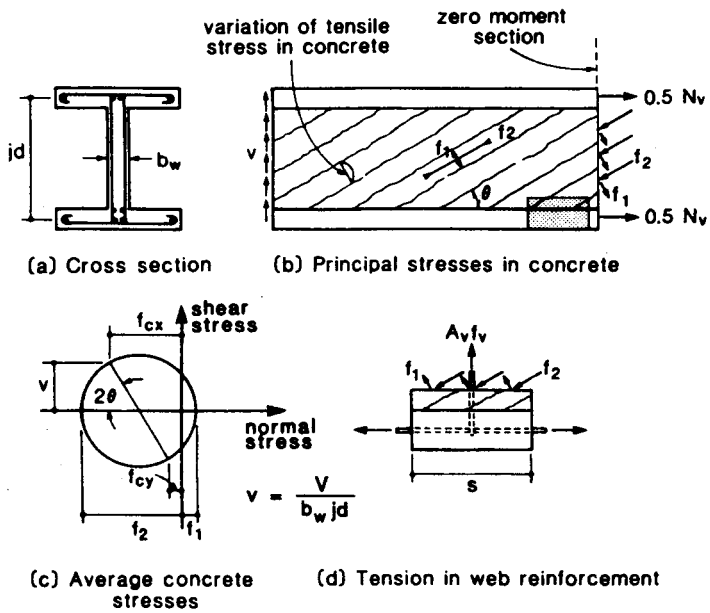

Figure 7-35 Equilibrium conditions of modified compression field theory.

where f_v is the average stress in the stirrups. Substituting for f_2 from Eq. (7-27) gives

$$V = f_1 b_w jd \cot\theta + \frac{A_v f_v}{s} jd \cot\theta \tag{7-28}$$

Equation (7-28) expresses the shear resistance of a member as the sum of a concrete contribution, which depends on tensile stresses in the concrete, and a steel contribution, which depends on tensile stresses in the stirrups. That is, it has the same form as the ACI shear equation $V_c + V_s$.

If the axial load on the member is zero, the unbalanced longitudinal component of the diagonal concrete stresses must be equilibrated by tensile stresses in the longitudinal reinforcement. This longitudinal equilibrium requirement can be expressed as

$$A_{sx} f_\ell + A_{px} f_p = (f_2 \cos^2\theta - f_1 \sin^2\theta) b_w jd$$

where f_ℓ and f_p are the average stresses in the longitudinal reinforcing bars and longitudinal prestressing steel. Substituting for f_2 from Eq. (7-27) gives

$$A_{sx} f_\ell + A_{px} f_p = V \cot\theta - f_1 b_w jd \tag{7-29}$$

Based on their tests of reinforced concrete panels in pure shear, Vecchio and Collins (Ref. 7-36) recommended the average tensile stress vs. average tensile strain relationship illustrated in Fig. 7-36.

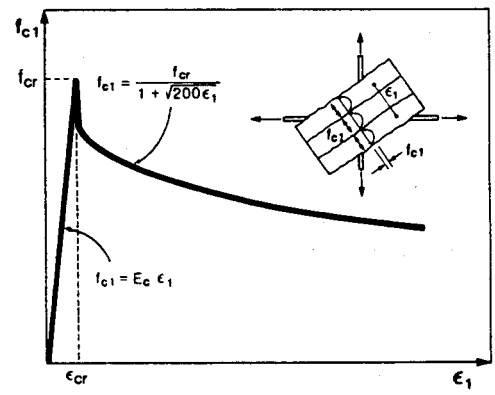

(a) Average stress-strain relationship for cracked concrete in tension

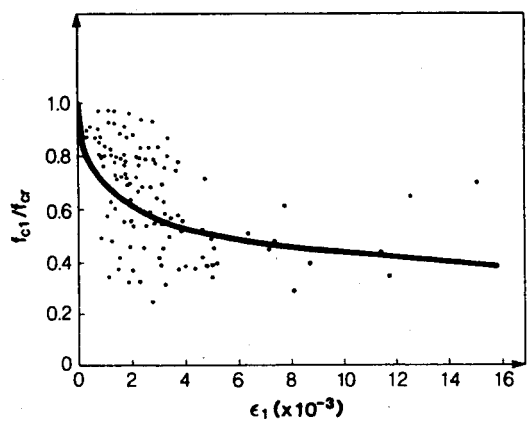

(b) Correlation of test data for cracked concrete in tension

Figure 7-36 Tensile stress-strain relationship for diagonally cracked concrete.

To be consistent with the expression used in Section 4.10, it is recommended that the following relationships be used

$$\text{if} \quad \epsilon_1 \leq \epsilon_{cr} \qquad \text{then} \qquad f_1 = E_c\,\epsilon_1 \tag{7-30}$$

$$\epsilon_1 > \epsilon_{cr} \qquad \text{then} \qquad f_1 = \frac{\alpha_1 \alpha_2 f_{cr}}{1 + \sqrt{500\epsilon_1}} \tag{7-31}$$

where α_1 and α_2 are factors accounting for the bond characteristics of the reinforcement and the type of loading (see Section 4.10).

In the treatment above we have considered average stresses and average strains and have not dealt with local variations. The stresses that occur at a crack location will differ from the calculated average values (see Fig. 7-37). At a crack the tensile stress in the concrete goes to zero, while the tensile stresses in the reinforcement become larger. The shear capacity of the member may be limited by the ability of the member to transmit forces across the crack.

At low shear values, tension is transmitted across the crack by local increases in reinforcement stresses. At a certain shear force the stress in the web reinforcement will just reach yield at the crack locations. At higher shear forces transmitting tension across the crack will require local shear stresses, v_{ci}, on the crack surface (see Fig. 7-37c).

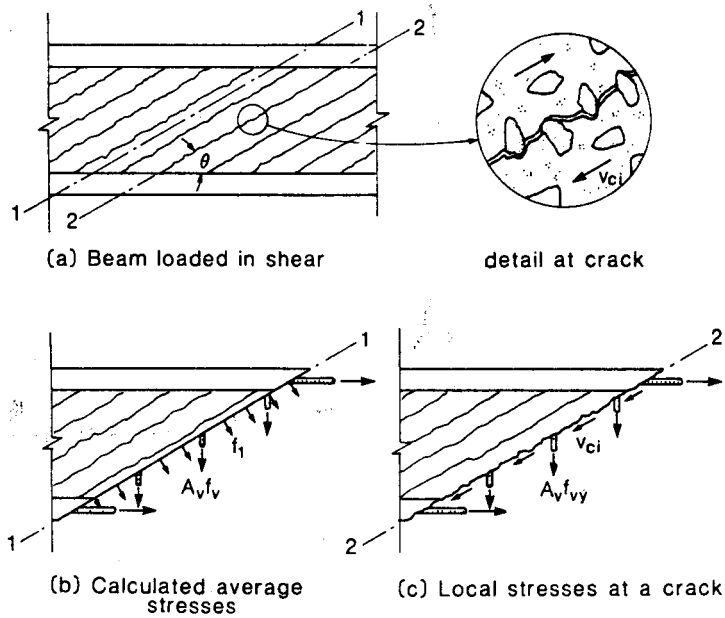

Figure 7-37 Transmitting forces across cracks.

The ability of the crack interface to transmit these shear stresses will depend on the crack width, w. It is suggested that the limiting value of v_{ci} be taken as

$$v_{ci} = \frac{2.16\sqrt{f'_c}}{0.3 + \dfrac{24w}{a + 0.63}} \quad \text{psi and in.} \tag{7-32a}$$

$$v_{ci} = \frac{0.18\sqrt{f'_c}}{0.3 + \dfrac{24w}{a + 16}} \quad \text{MPa and mm} \tag{7-32b}$$

where a is the maximum aggregate size. The expression above has been simplified from the expressions developed by Vecchio and Collins (Ref. 7-36) using the experimental data of Walraven (Ref. 7-37). In the expression above the beneficial effects of local compressive stresses across the crack have been ignored.

The two sets of stresses shown in Fig. 7-37b and c must be statically equivalent. The requirement that the two sets of stresses produce the same vertical force is

$$A_v f_v \left(\frac{jd}{s \tan\theta}\right) + f_1 \frac{b_w jd}{\sin\theta} \cos\theta = A_v f_{vy} \left(\frac{jd}{s \tan\theta}\right) + v_{ci}\, b_w jd$$

and hence, to maintain this equality, f_1 must be limited to

$$f_1 = v_{ci} \tan\theta + \frac{A_v}{s b_v}(f_{vy} - f_v) \tag{7-33}$$

where v_{ci} is given by Eq. (7-32).

The crack width, w, to be used in Eq. (7-32) can be taken as the product of the principal tensile strain, ϵ_1, and the average spacing of the diagonal cracks. Thus

$$w = \epsilon_1 s_{m\theta} \tag{7-34}$$

The spacing of the inclined cracks will depend upon the crack control characteristics of both the longitudinal and the transverse reinforcement. It is suggested that this spacing be taken as

$$s_{m\theta} = 1 \Big/ \left(\frac{\sin\theta}{s_{mx}} + \frac{\cos\theta}{s_{mv}}\right) \tag{7-35}$$

where s_{mx} and s_{mv} are the crack spacings indicative of the crack control characteristics of the longitudinal and transverse reinforcement, respectively (see Fig. 7-38). Thus s_{mx} is the average crack spacing that would result if the member was subjected to longitudinal tension while s_{mv} is the average crack spacing that would result if the member was subjected to a transverse tension.

These crack spacings can be estimated from the CEB-FIP Code (Ref. 7-28) crack spacing expression, Eq. (4-23). The CEB expression was intended to calculate crack spacings on the surface of the member. For use in Eq. (7-32) it is crack spacings in the shear area of the beam that are of interest. To account for the fact that crack spacings become larger as the distance from the reinforcement increases, the maximum distance from the reinforcement, instead of the cover distance c, will be used (see Fig. 7-39). Thus, for the uniform tensile straining (i.e., $k_2 = 0.25$), Eq. (4-23) becomes

$$s_{mx} = 2\left(c_x + \frac{s_x}{10}\right) + 0.25 k_1 \frac{d_{bx}}{\rho_x} \tag{7-36}$$

$$s_{mv} = 2\left(c_v + \frac{s}{10}\right) + 0.25 k_1 \frac{d_{bv}}{\rho_v} \tag{7-37}$$

where $\rho_v = A_v/(b_w s)$ and $\rho_x = (A_{sx} + A_{px})/A_c$, and k_1 is 0.4 for deformed bars or 0.8 for plain bars or bonded strands.

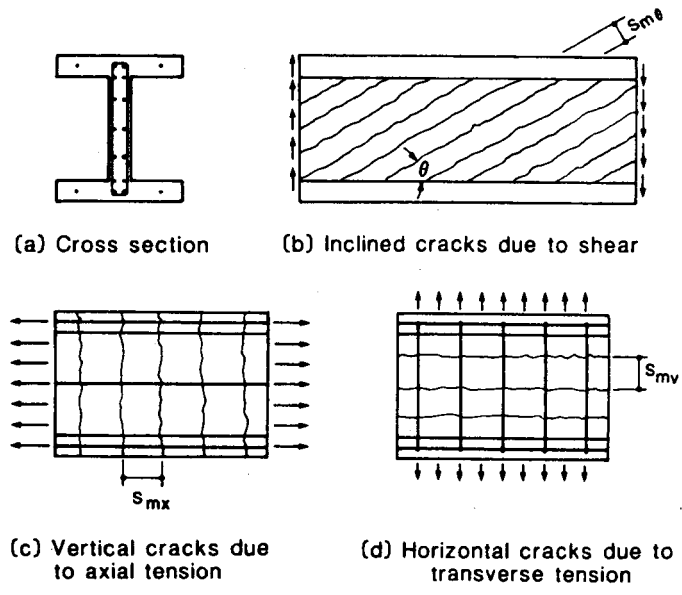

Figure 7-38 Spacing of inclined cracks.

Yielding of the longitudinal reinforcement at a crack may also limit the magnitude of concrete tension that can be transmitted. The requirement that the two sets of stresses in Fig. 7-37 produce the same horizontal force will be satisfied if

$$A_{sx} f_y + A_{px} f_{ps} \geq A_{sx} f_{sx} + A_{px} f_{px} + f_1 b_w jd + \left[f_1 - \frac{A_v}{b_w s}(f_{vy} - f_v) \right] b_w jd \cot^2 \theta \tag{7-38}$$

All of the relationships needed to predict the response of a beam loaded in shear have been discussed above. A suitable solution technique for using these relationships is as follows:

Step 1: Choose a value of ϵ_1 at which to perform the calculations.
Step 2: Estimate θ.
Step 3: Calculate w from Eqs. (7-34), (7-35), (7-36), and (7-37).
Step 4: Estimate f_v.
Step 5: Calculate f_1 from Eqs. (7-31) and (7-33) and take the smaller value.
Step 6: Calculate V from Eq. (7-28).
Step 7: Calculate f_2 from Eq. (7-27).
Step 8: Calculate f_{2max} from Eq. (7-26).
Step 9: Check that $f_2 \leq f_{2max}$.
If $f_2 > f_{2max}$, solution is not possible. Return to Step 1 and choose a smaller ϵ_1.

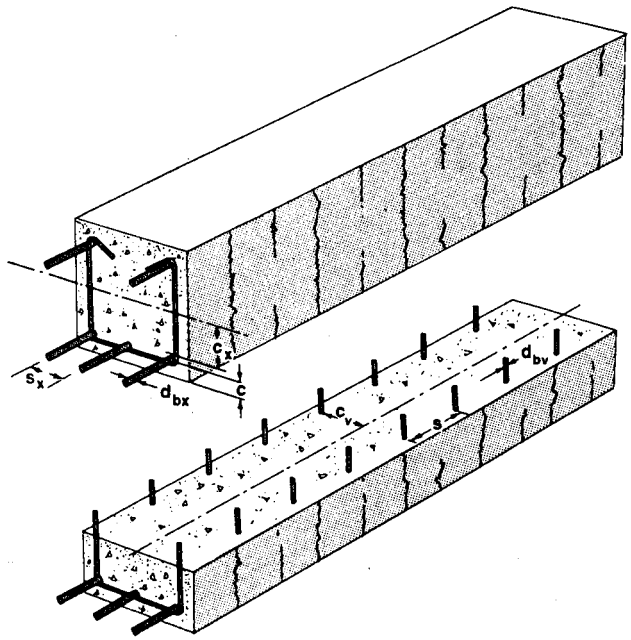

Figure 7-39 Parameters influencing crack spacing.

Step 10: Calculate $\epsilon_2 = \epsilon_c' \left(1 - \sqrt{1 - f_2/f_{2max}}\right)$ ... from Eq. (7-26).

Step 11: Calculate ϵ_x and ϵ_t from Eqs. (7-23) and (7-24) as

$$\epsilon_x = \frac{\epsilon_1 \tan^2 \theta + \epsilon_2}{1 + \tan^2 \theta}$$

$$\epsilon_t = \frac{\epsilon_1 + \epsilon_2 \tan^2 \theta}{1 + \tan^2 \theta}$$

Step 12: Calculate $f_v = E_s \epsilon_t \leq f_{vy}$.

Step 13: Check estimate of f_v. If necessary, revise estimate and return to Step 5.

Step 14: Calculate $f_{sx} = E_s \epsilon_x \leq f_y$ and $f_p = E_p(\epsilon_x + \Delta\epsilon_p) \leq f_{py}$.

Step 15: Calculate the axial force on the member.

$$N = A_{sx} f_{sx} + A_{px} f_p - \frac{V}{\tan \theta} + f_1 b_w j d - f_c(A_c - b_w j d)$$

where f_c is the axial compressive stress in the concrete areas outside the web.

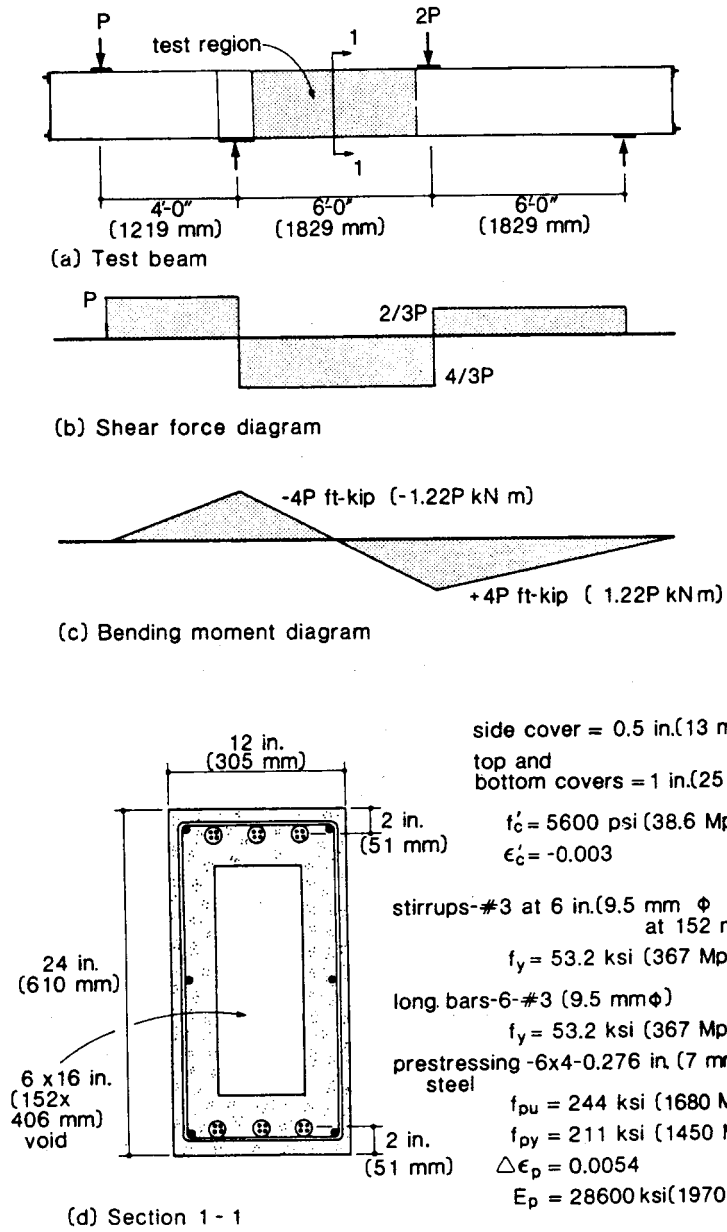

Figure 7-40 Details of beam CF1 tested by Arbesman and Conte (Ref. 7-38).

If ϵ_x is tensile then $f_c = 0$, otherwise,

$$f_c = f'_c \left[2\left(\frac{\epsilon_x}{\epsilon'_c}\right) - \left(\frac{\epsilon_x}{\epsilon'_c}\right)^2 \right]$$

Step 16: Check the axial load. If N is not equal to the desired value (usually zero), make a new estimate of θ and return to Step 2. Increasing θ increases N.

Step 17: Check that the longitudinal reinforcement can carry stresses across the crack, using Eq. (7-38). If this requirement is not satisfied, we must lower f_1 and return to Step 6.

To obtain the complete response of the beam, these calculations are repeated for a range of values of ϵ_1 starting from the cracking strain ($\epsilon_1 \approx 0.1 \times 10^{-3}$) and increasing ϵ_1 until the shear has reached its maximum value. A short computer program called SHEAR, based on the calculation procedure above, is described in Appendix B.

7.11 EXAMPLE OF PREDICTING RESPONSE IN SHEAR

In order to illustrate the procedure that can be used to predict the load-deformation response of a prestressed concrete member subjected to shear, we will consider the member described in Fig. 7-40. This symmetrically reinforced post-tensioned box beam was loaded so that a point of zero moment occurred midway along the test length. We wish to determine the relationship between the applied shear and the strains in the stirrups.

To determine the complete shear force–stirrup strain response, we will determine the shears and stirrup strains that correspond to various values of the principal tensile strain, ϵ_1. The procedure is described in Section 7.10.

The response of this beam at the location of zero moment can be determined using program SHEAR described in Appendix B. In using this program we must input the crack spacing parameters s_{mx} and s_{mv}. As the longitudinal reinforcement consists of both bonded wires ($k_1 = 0.8$) and deformed bars ($k_1 = 0.4$) it is appropriate to use a weighted average for k_1 when calculating s_{mx}. Thus

$$k_1 = \frac{0.4 \times 0.66 + 0.8 \times 1.436}{0.66 + 1.436}$$
$$= 0.67$$

Hence

$$s_{mx} = 2\left(5.05 + \frac{2.5}{10}\right) + \frac{0.25 \times 0.67 \times 0.375}{(0.66 + 1.436)/192} = 16.3 \text{ in. } (414 \text{ mm})$$

The crack-control parameter in the y-direction is

$$s_{mv} = 2\left(2.125 + \frac{6}{10}\right) + \frac{0.25 \times 0.4 \times 0.375}{0.22/(6 \times 6)} = 11.6 \text{ in. } (295 \text{ mm})$$

The results obtained by using program SHEAR are given in Table 7-2.

Table 7-2 Summary of shear response predictions for beam CF1 using the modified compression field theory.

ϵ_1 $\times 10^3$	θ deg.	ϵ_t $\times 10^3$	ϵ_x $\times 10^3$	γ $\times 10^3$	f_2 ksi (MPa)	f_{2max} ksi (MPa)	f_1 psi (MPa)	w in. (mm)	V kips (kN)	Comments
0.01	10.5	0	−0.30	0.11	1.10	5.60	37	0.000	24.3	
					(7.6)	(38.6)	(0.3)	(0)	(108)	
0.08	25.2	0	−0.30	0.36	1.35	5.60	299	0.001	76.2	Cracking
					(9.3)	(38.6)	(2.1)	(0.03)	(339)	
0.5	23.7	0.35	−0.26	0.67	1.42	5.60	200	0.005	71.5	
					(9.8)	(38.6)	(1.4)	(0.13)	(318)	
1.0	24.6	0.75	−0.21	1.11	1.60	5.60	176	0.010	80.5	
					(11.0)	(38.6)	(1.2)	(0.25)	(358)	
1.5	25.4	1.13	−0.15	1.57	1.79	5.60	161	0.014	91.0	
					(12.3)	(38.6)	(1.1)	(0.36)	(405)	
2.0	26.1	1.49	−0.10	2.06	1.99	5.46	150	0.019	101.4	
					(13.7)	(37.6)	(1.0)	(0.48)	(451)	
2.5	26.3	1.87	−0.06	2.56	2.11	5.17	110	0.024	105.7	Stirrups yield and
					(14.5)	(35.6)	(0.8)	(0.61)	(470)	crack slipping
3.0	25.7	2.30	−0.04	2.93	2.15	4.91	96	0.029	105.1	
					(14.8)	(33.9)	(0.7)	(0.74)	(468)	
4.0	24.8	3.15	−0.01	3.70	2.21	4.47	76	0.038	104.4	
					(15.3)	(30.8)	(0.5)	(0.97)	(464)	
6.0	23.9	4.84	0.07	5.26	2.26	3.78	54	0.058	102.8	
					(15.6)	(26.1)	(0.4)	(1.47)	(457)	
8.0	23.4	6.52	0.13	6.82	2.28	3.28	42	0.077	101.7	
					(15.7)	(22.6)	(0.3)	(1.96)	(452)	
10.0	23.2	8.20	0.17	8.41	2.29	2.90	35	0.097	100.9	
					(15.8)	(20.0)	(0.2)	(2.46)	(449)	
14.0	23.1	11.48	0.12	11.84	2.26	2.35	26	0.135	98.8	Concrete crushing
					(15.6)	(16.2)	(0.2)	(3.43)	(439)	

Figure 7-41 compares the predicted and measured stirrup strains for this beam. Note that for shears less than the diagonal cracking shear the stirrup strains are negligibly small, a phenomenon correctly predicted by the modified compression field theory. The growth in stirrup strain after diagonal cracking is predicted well by the theory. Also shown in Fig. 7-41 is the response predicted using the compression field theory, which can be obtained by inputting a value of zero for the cracking strength of the concrete.

It can be seen from Fig. 7-41 that by accounting for the tensile stresses in the cracked concrete, we have more accurately predicted the response of the prestressed concrete member. As can be seen from Table 7-2, after cracking, the principal tensile stress, f_1, in the concrete decreases with increasing values of ϵ_1. For this example, the ability of the crack to transmit shear limited f_1 at higher values of ϵ_1.

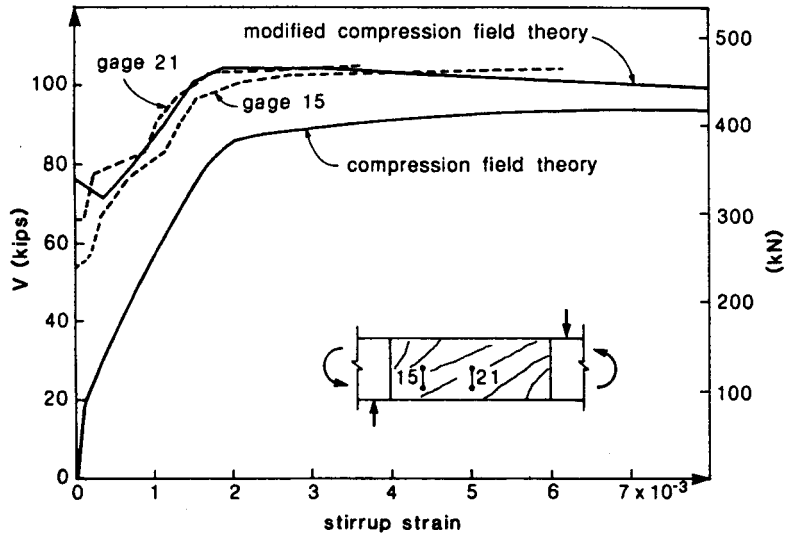

Figure 7-41 Comparison of measured stirrup strains and predicted stirrup strains for beam CF1.

It is interesting to note that for this prestressed concrete member, the inclination, θ, of the principal compressive stresses starts at zero when the shear is zero (i.e., the principal compressive stresses due to prestressing are longitudinal). As shear is increased, the principal compressive stresses become more steeply inclined reaching a maximum of about 26° as the stirrups yield. The very flat inclination of the diagonal compressive stresses means that the diagonal cracks form at small angles as can be seen in Fig. 7-42.

In predicting the response of beam CF1 shown above, it was assumed that the member was subjected to pure shear. While the moment was zero at a section midway along the test length (see Fig. 7-40), other sections in the test length were subjected to significant flexure. The presence of flexure reduced somewhat the shear capacity of the beam, and hence failure was initiated in the higher moment regions.

Under the combined action of shear and moment, the longitudinal strains vary over the depth of the beam (see Fig. 7-43). Vecchio and Collins (Ref. 7-39) have shown how it is possible to perform a detailed analysis of a cross section subjected to combined shear and moment. By considering two adjacent cross sections they are able to calculate the distribution of shear stresses over the cross section. In this analysis, the biaxial stresses and strains and the manner in which they vary over the height of the beam are considered. It is found that the inclination, θ, of the principal compressive stress changes over the height of the beam, becoming larger near the flexural tension face and smaller near the flexural compression face (see Fig. 7-43a).

The detailed, dual-section analysis is very time consuming. It is possible to greatly reduce the computation time if the following simplifications are adopted:

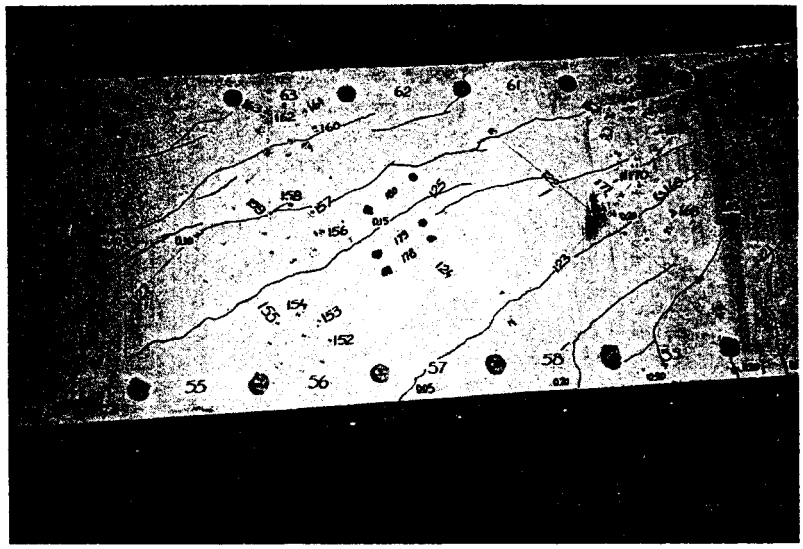

Figure 7-42 Crack pattern near failure load of prestressed beam CF1.

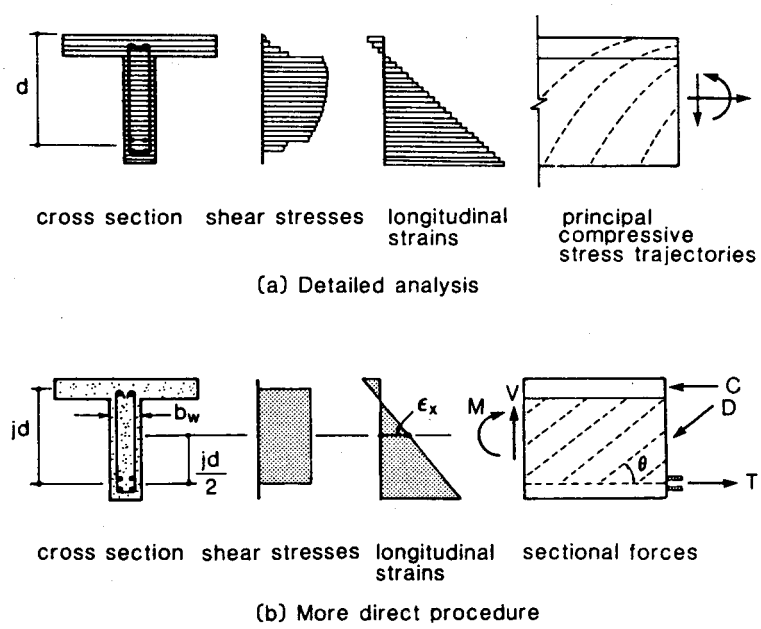

Figure 7-43 Influence of moment on shear response.

1. The redistribution of shear stresses that occurs at higher moments is ignored. That is, the shear stress is assumed to be given by Eq. (7-5) (see Fig. 7-43b).
2. The biaxial stresses and strains are considered at just one level of the web. The longitudinal strain at this location, ϵ_x, is used to calculate θ, which is then assumed to remain constant over the depth of the web (see Fig. 7-43b).

With this simplified procedure a suitable solution technique for analyzing a section subjected to combined shear and moment is as follows:

Steps 1 through **13:** Identical to the steps for pure shear given in Section 7.10.

Step 14: Using a plane-sections analysis with the strain at the chosen level set to the ϵ_x value calculated in Step 11, find the strain distribution that corresponds to the desired moment and then determine the corresponding axial load, N_p.

Step 15: Calculate the axial force on the member, allowing for the influence of the longitudinal compressive stresses in the concrete over area $b_w jd$ caused by the shear

$$N = N_p - V \cot \theta$$

Step 16: Check whether N equals the desired axial load on the member. If it does not, make a new estimate of θ and return to Step 3. Increasing θ increases N.

The procedure above has been incorporated into program RESPONSE (described in Appendix A), which can be used to predict the response of sections subjected to combined shear, moment, and axial load.

Before this procedure can be used, a decision must be made as to where in the web ϵ_x will be calculated. As an increase in ϵ_x decreases the shear capacity, it would be conservative to use the highest value of ϵ_x. However, members with web reinforcement have a considerable capacity for redistribution, which results in the shear stresses being transferred from the most highly strained portions of the cross section to the less highly strained portions. Because of this redistribution, it is reasonable to use the longitudinal strain at mid-depth of the web as ϵ_x. Members that do not contain web reinforcement have less capacity for redistribution and hence, for such members the highest longitudinal strain in the web should be used as ϵ_x.

Figure 7-44 compares the shear-moment interaction diagram for beam CF1 obtained from program RESPONSE with that obtained from the more detailed dual-section analysis. Note that even though ϵ_x was taken as the longitudinal strain at mid-depth of the web, the failure envelope predicted by program RESPONSE is more conservative than that given by the dual-section analysis. Also shown in Fig. 7-44 is the shear stress distribution at one point on the failure envelope predicted by the dual-section analysis. The significant redistribution of shear stresses across the section that has occurred, can be seen.

Flexure reduces the shear capacity of beam CF1 because it increases the longitudinal strain, ϵ_x. As this strain increases, shear capacity decreases. Recognizing the key role played by the longitudinal strain enables us to develop a simple method of accounting for the influence of flexure on shear capacity.

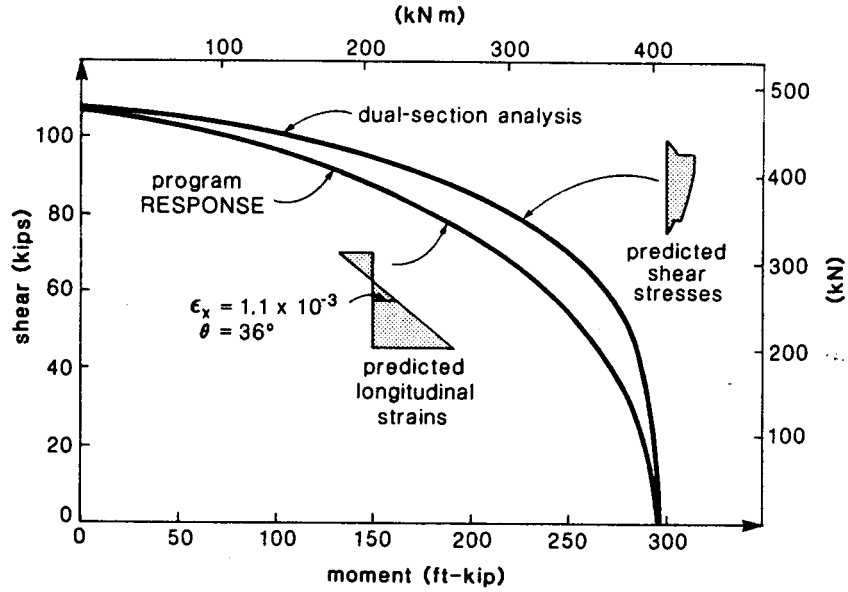

Figure 7-44 Shear-moment interaction diagrams for beam CF1 predicted by program RESPONSE and by a dual-section analysis.

For the non-prestressed section shown in Fig. 7-45 the applied moment, if acting alone, would cause a tensile strain in the reinforcement of

$$\epsilon_x = \frac{M}{jd\,A_s E_s} \tag{7-39}$$

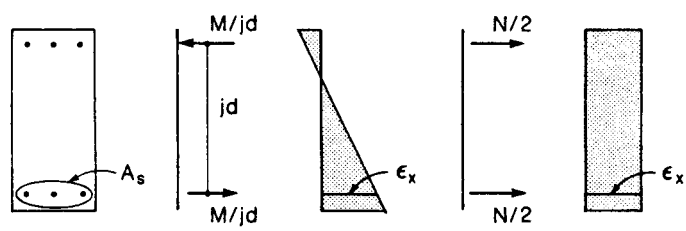

(a) Cross section (b) Forces and strains due to moment M (c) Forces and strains due to tension N

Figure 7-45 Comparison of forces and strains due to moment and tension.

If the section was subjected to a pure axial tension, the tensile strain in the reinforcement would be

$$\epsilon_x = \frac{0.5N}{A_s E_s} \tag{7-40}$$

Comparing Eqs. (7-39) and (7-40) we see that to produce the same longitudinal strain with an axial force as with a moment, the magnitude of the axial force must be

$$N = \frac{2M}{jd} \tag{7-41}$$

Thus, if beam CF1 is subjected to a moment of 200 ft-kips (271 kNm) it will have the same shear capacity as if it was subjected to an axial tension of

$$N = \frac{2 \times 200 \times 12}{20} = 240 \text{ kips } (1068 \text{ kN})$$

If beam CF1 is analyzed using program SHEAR, for combined shear and axial tension, with a constant axial tension of 240 kips (1068 kN) it will be found that the shear capacity is predicted to be 75.0 kips (334 kN). It can be seen from Fig. 7-44 that this predicted shear capacity agrees well with the shear capacity predicted by program RESPONSE for the case of beam CF1 subjected to a moment of 200 ft-kips (271 kNm).

7.12 DESIGN USING MODIFIED COMPRESSION FIELD THEORY

The modified compression field theory was presented in the previous sections as an analysis method capable of predicting the response of a particular section of a prestressed concrete member when that section was subjected to combined shear, axial load, and moment. With the aid of a suitable computer program, such as program RESPONSE or SHEAR, this method can be used to evaluate the suitability of a chosen section and hence can be used to design sections for shear.

By making some simplifying assumptions it is possible to rearrange the basic equations of the modified compression field theory so that they can be used in a more direct fashion to design a section subjected to combined shear, axial load, and flexure.

Typically, before design for shear commences, the cross-sectional dimensions, prestressing and material strengths have all been chosen to satisfy other design considerations. Shear design then reduces to checking that the cross-sectional dimensions are adequate and finding the required amounts of web reinforcement and additional longitudinal reinforcement that will ensure that the required shear strength of the section can be developed.

The nominal shear resistance of a section can be expressed as

$$V_n = V_c + V_s + V_p \tag{7-42}$$

where V_c is the nominal shear strength provided by tensile stresses in the concrete, V_s is the nominal shear strength provided by tensile stresses in the web reinforcement, and V_p is the nominal shear strength provided by the component in the direction of the applied shear, of the force in the longitudinal prestressing tendons.

The shear resisted by tensile stresses in the concrete can be expressed as

$$V_c = \beta \sqrt{f'_c} b_w jd \tag{7-43}$$

where jd equals the flexural lever arm, which need not be taken less than $0.9d$. For prestressed members, d need not be taken less than $0.8h$. The factor β depends on the average tensile stresses in the cracked concrete. Assuming that the cracking stress, f_{cr}, equals $4\sqrt{f'_c}$ psi ($0.33\sqrt{f'_c}$ MPa) Eqs. (7-28) and (7-31) can be rearranged to give

$$\beta = \frac{\alpha_1 \alpha_2 \, 4 \cot\theta}{1 + \sqrt{500\epsilon_1}} \qquad \text{psi} \tag{7-44a}$$

$$\beta = \frac{\alpha_1 \alpha_2 \, 0.33 \cot\theta}{1 + \sqrt{500\epsilon_1}} \qquad \text{MPa} \tag{7-44b}$$

If the crack widths are too wide, the average tension in the concrete will be limited by the mechanisms that transmit the forces across the cracks. In particular, the shear stress on the crack, v_{ci}, will become critical. To avoid such "crack slipping" failures, β must be limited to

$$\beta \leq \frac{2.16}{0.3 + \dfrac{24\epsilon_1 s_{m\theta}}{a + 0.63}} \qquad \text{psi and in.} \tag{7-45a}$$

$$\beta \leq \frac{0.18}{0.3 + \dfrac{24\epsilon_1 s_{m\theta}}{a + 16}} \qquad \text{MPa and mm} \tag{7-45b}$$

Equation (7-45) was derived from Eqs. (7-28), (7-32), (7-33), and (7-34). It was assumed that the stirrups would be yielding at failure ($f_v = f_{vy}$).

It can be seen from both of the above expressions for β that as the tensile straining of the concrete increases (i.e., ϵ_1 increases), the shear that can be resisted by tensile stresses in the concrete, V_c, decreases. The value of the principal tensile strain, ϵ_1, will depend on the magnitude of the longitudinal tensile straining, ϵ_x, the inclination, θ, of the principal stresses , and the magnitude of the principal compressive strain, ϵ_2, in the concrete. From Eqs. (7-23) and (7-24), ϵ_1 is

$$\epsilon_1 = \epsilon_x + (\epsilon_x - \epsilon_2)\cot^2\theta \tag{7-46}$$

The strain ϵ_2 depends upon the magnitude of the principal compressive stress, f_2. This stress can be estimated conservatively from Eq. (7-27) as

$$f_2 = (\tan\theta + \cot\theta)v \tag{7-47}$$

Assuming that the strain, ϵ'_c, at which the concrete reaches its peak stress is -0.002, we can rearrange Eq. (7-26) to give

$$\epsilon_2 = -0.002\left(1 - \sqrt{1 - f_2/f_{2max}}\right) \tag{7-48}$$

where

$$f_{2max} = \frac{f'_c}{0.8 + 170\epsilon_1} \tag{7-49}$$

If we substitute the expression for ϵ_2 given by Eq. (7-48) into Eq. (7-46) and in addition, substitute the expressions for f_2 and f_{2max} from Eqs. (7-47) and (7-49) we obtain the following quadratic equation for ϵ_1

$$\epsilon_1 = \epsilon_x + \left[\epsilon_x + 0.002\left(1 - \sqrt{1 - \frac{v}{f'_c}(\tan\theta + \cot\theta)(0.8 + 170\epsilon_1)}\right)\right]\cot^2\theta \qquad (7\text{-}50)$$

Thus, if ϵ_x, θ, and v/f'_c are known, the strain, ϵ_1, can be found by solving Eq. (7-50). With ϵ_1 known, the β factor can be calculated from Eqs. (7-44) and (7-45) provided that the crack spacing, $s_{m\theta}$, the maximum aggregate size, a, and the tension-stiffening factors, $\alpha_1\alpha_2$, are known.

To simplify the calculations we will assume that for members with web reinforcement, the crack spacing, $s_{m\theta}$, equals 12 in. (305 mm), that $\alpha_1\alpha_2$ equals unity, and that a equals 0.75 in. (19 mm). For the values of $v/f'_c, \epsilon_x$, and θ given in Table 7-3, the values of β calculated from the approach above are listed. In using this table, the nominal shear stress on the concrete is computed as

$$v = \frac{V_n - V_p}{b_w j d} \qquad (7\text{-}51)$$

Table 7-3 Values of θ and β, psi units*, for members with web reinforcement.

Shear Stress v/f'_c		Longitudinal Strain $\epsilon_x \times 1000$									
		0	0.25	0.50	0.75	1.00	1.50	2.00	2.50	3.00	5.00
≤ 0.050	θ	28°	31°	34°	36°	38°	41°	43°	45°	46°	56°
	β	5.24	3.70	3.01	2.62	2.33	1.95	1.72	1.54	1.39	0.92
0.075	θ	28°	30°	30°	34°	36°	40°	42°	43°	43°	56°
	β	4.86	3.37	2.48	2.37	2.15	1.90	1.65	1.44	1.25	0.92
0.100	θ	22°	26°	30°	34°	36°	38°	38°	38°	38°	55°
	β	2.71	2.42	2.31	2.27	2.08	1.72	1.39	1.16	1.00	0.95
0.125	θ	23°	27°	31°	34°	36°	36°	36°	36°	36°	55°
	β	2.40	2.33	2.29	2.16	2.00	1.52	1.23	1.03	0.88	0.94
0.150	θ	25°	28°	31°	34°	34°	34°	34°	34°	35°	55°
	β	2.53	2.25	2.13	2.06	1.73	1.30	1.04	0.85	0.77	0.94
0.175	θ	26°	29°	32°	32°	32°	32°	34°	36°	38°	54°
	β	2.34	2.19	2.11	1.69	1.40	1.01	0.94	0.91	0.88	0.96
0.200	θ	27°	30°	33°	34°	34°	34°	37°	39°	41°	53°
	β	2.16	2.13	2.09	1.82	1.52	1.08	1.11	1.04	0.99	0.98
0.225	θ	28°	31°	34°	34°	34°	37°	39°	42°	44°	–
	β	1.97	2.07	2.08	1.67	1.35	1.29	1.17	1.16	1.09	–
0.250	θ	30°	32°	34°	35°	36°	39°	42°	45°	49°	–
	β	2.26	2.00	1.87	1.63	1.45	1.37	1.32	1.28	1.24	–

*For β values in MPa units, divide the values given in the table by 12.

The shear resisted by tensile stresses in the web reinforcement can be determined from Eq. (7-28) as

$$V_s = \frac{A_v f_y jd \cot\theta}{s} \tag{7-52}$$

It can be seen from Eq. (7-52) that for a given quantity of stirrups, the lower the value of θ, the higher the value of V_s. However, for a given value of ϵ_x, lower values of θ will result in higher values of ϵ_1 [see Eq. (7-50)], and hence lower values of V_c.

The θ values given in Table 7-3 have been chosen to ensure that, for highly stressed members, the compressive stress in the concrete, f_2, does not exceed the crushing strength, f_{2max} and that the strain in the web reinforcement, ϵ_v, is at least equal to 0.002. Within the possible range of values of θ, the values given in the table will result in close to the minimum amount of shear reinforcement.

To be conservative, the longitudinal strain, ϵ_x, will be taken at the level of the flexural tension reinforcement. This strain will depend upon the magnitude of the flexural moment, the axial tension (see Fig. 7-45) and the shear (see Fig. 7-23) as well as the amount of non-prestressed and prestressed longitudinal reinforcement. It may be computed as

$$\epsilon_x = \frac{\frac{M_u}{jd} + 0.5N_u + 0.5V_u \cot\theta - A_{ps} f_{se}}{E_s A_s + E_p A_{ps}} \tag{7-53}$$

Equation (7-53) neglects the stiffness of the concrete when calculating strain. While this is reasonable for tensile strains, it will not be appropriate for compressive strains. Hence, if ϵ_x given by Eq. (7-53) is negative, the value will be overestimated. In this case it will be conservative to take ϵ_x as equal to zero.

Because the amount of longitudinal reinforcement provided must be sufficient to avoid yielding of the reinforcement, a simple, conservative procedure for calculating ϵ_x is to estimate the concrete strain associated with yielding of the reinforcement. That is,

$$\epsilon_x \leq \frac{f_y}{E_s} \tag{7-54}$$

and

$$\epsilon_x \leq \frac{f_{py} - f_{se}}{E_p} \tag{7-55}$$

Carrying part of the shear by tensile stresses in the concrete reduces the required amount of web reinforcement but increases the stresses in the longitudinal reinforcement at a crack [see Fig. 7-37c and Eq. (7-38)].

The force in the longitudinal reinforcement at a crack caused by shear can be determined from Eq. (7-38). Substituting for the average reinforcement force $A_{sx} f_{sx} + A_{px} f_{px}$ from Eq. (7-29) and assuming the stirrups are yielding ($f_v = f_{vy}$) enables Eq. (7-38) to be written as

$$A_{sx} f_y + A_{px} f_{ps} \geq V \cot\theta + f_1 b_w jd \cot^2\theta \tag{7-56}$$

But from Eq. (7-28)

$$V_c = f_1 b_w jd \cot\theta \tag{7-57}$$

Hence Eq. (7-56) can be written as

$$A_{sx}f_y + A_{px}f_{ps} \geq V\cot\theta + V_c\cot\theta \tag{7-58}$$

For the symmetrically reinforced member considered in deriving Eq. (7-38)

$$V = V_c + V_s$$

Thus Eq. (7-58) can be expressed as

$$A_{sx}f_y + A_{px}f_{ps} \geq (2V_c + V_s)\cot\theta \tag{7-59}$$

Considering only the reinforcement on the flexural tension side of the member enables Eq. (7-59) to be written as

$$A_s f_y + A_{ps}f_{ps} \geq (V_c + 0.5V_s)\cot\theta \tag{7-60}$$

But, from Eq. (7-42),

$$V_c + 0.5V_s = V_n - 0.5V_s - V_p$$

Hence the force in the longitudinal tension reinforcement caused by shear can be expressed as

$$A_s f_y + A_{ps}f_{ps} \geq \left(\frac{V_u}{\phi} - 0.5V_s - V_p\right)\cot\theta \tag{7-61}$$

Thus to avoid yielding of the longitudinal reinforcement, for combined loading the reinforcement on the flexural tension face must be proportioned so that

$$A_s f_y + A_{ps}f_{ps} \geq \frac{M_u}{\phi jd} + 0.5\frac{N_u}{\phi} + \left(\frac{V_u}{\phi} - 0.5V_s - V_p\right)\cot\theta \tag{7-62}$$

Thus the shear design of a member containing web reinforcement consists of the following steps:

Step 1: Calculate the nominal shear stress, v, from Eq. (7-51) and divide by the concrete strength, f'_c, to obtain the shear stress ratio, v/f'_c. If this ratio is higher than 0.25 the section is too small, or the concrete is too weak.

Step 2: Calculate the longitudinal strain, ϵ_x, either directly from Eqs. (7-54) and (7-55) or by trial and error from Eq. (7-53), where an estimate of θ will be required.

Step 3: Using the calculated values of v/f'_c and ϵ_x determine θ and β from Table 7-3. Linear interpolation can be used or the values given for the next higher value of ϵ_x and the next higher value of v/f'_c can be taken.

Step 4: Calculate the required value of V_s from Eqs. (7-42) and (7-43) as

$$V_s = \frac{V_u}{\phi} - V_p - \beta\sqrt{f'_c}b_w jd \tag{7-63}$$

Step 5: Calculate the required spacing of stirrups from Eq. (7-52) as

$$s \leq \frac{A_v f_y jd \cot\theta}{V_s} \tag{7-64}$$

Step 6: Check yielding of the longitudinal reinforcement using Eq. (7-62). If needed, either add more longitudinal reinforcement or revise the values of θ and β using the values for a higher ϵ_x. These values will reduce the amount of longitudinal reinforcement but increase the amount of stirrups required.

Because the procedure above was based on the assumption that the member contained enough reinforcement to ensure reasonable crack control, irrespective of the crack direction, it is not appropriate to use this procedure for members that do not contain web reinforcement. Such members may have crack spacings, $s_{m\theta}$, considerably greater than the assumed value of 12 in. (305 mm). As can be seen from Eq. (7-37), if there is no web reinforcement (i.e., $\rho_v = 0$) the crack spacing becomes infinity.

If s_{mv} equals infinity then Eq. (7-35) becomes

$$s_{m\theta} = \frac{s_{mx}}{\sin\theta} \tag{7-65}$$

where s_{mx} is the spacing of vertical cracks (see Fig. 7-38).

For members without web reinforcement, the nominal shear resistance can be expressed as

$$V_n = V_c + V_p \tag{7-66}$$

Assuming that the crack spacing is given by Eq. (7-65), that $\alpha_1\alpha_2$ equals unity, and that the maximum aggregate size, a, equals 0.75 in. (19 mm), the values for β can be obtained from Eqs. (7-44), (7-45), and (7-50). These values are listed in Table 7-4. The values of θ given in the table are those that result in the highest value of β.

The crack spacing, s_{mx}, will be mainly influenced by the maximum distance from the reinforcement, c_x [see Eq. (7-36) and Fig. 7-39]. Rather than calculating s_{mx} from Eq. (7-36) we can determine it from the simple expressions given in Fig. 7-46. From this figure and from Table 7-4 it can be seen that as beams without web reinforcement become deeper, the shear stress required to cause failure becomes smaller.

Convincing evidence of the reduction in shear stress capacity that occurs as members become larger was provided by an extensive experimental program conducted in Japan by Shioya, Iguro, Nojiri, Akiyama, and Okada (Refs. 7-40 and 7-41). In this program, 13 beams having effective depths, d, ranging from 4 in. (100 mm) to 118 in. (3000 mm) were uniformly loaded until failure. As shown in Fig. 7-47, the shear stress required to cause failure decreased as d increased and decreased as the maximum aggregate size decreased. The largest beam in this series weighed nearly 500 tons and would have failed in shear under its own weight. The member was tested "upside down" by pressurizing a water-filled rubber bag between the specimen and a stronger reaction beam (see Fig. 7-48).

Table 7-4 Values of θ and β, psi units*, for members without web reinforcement.

Spacing Parameter s_{mx}		Longitudinal Strain $\epsilon_x \times 1000$									
		0	0.25	0.50	0.75	1.00	1.50	2.00	2.50	3.00	5.00
≤ 5 in.	θ	27°	30°	32°	33°	34°	36°	38°	39°	40°	43°
≤ 125 mm	β	4.89	3.74	3.19	2.81	2.55	2.19	1.95	1.77	1.63	1.27
10 in.	θ	30°	34°	37°	39°	41°	43°	45°	47°	48°	52°
250 mm	β	4.65	3.40	2.83	2.46	2.21	1.87	1.64	1.48	1.35	1.03
15 in.	θ	32°	37°	41°	43°	45°	48°	50°	52°	53°	58°
380 mm	β	4.47	3.15	2.59	2.23	1.99	1.67	1.45	1.30	1.17	0.87
25 in.	θ	35°	42°	46°	49°	51°	54°	57°	59°	61°	65°
630 mm	β	4.24	2.82	2.27	1.90	1.70	1.39	1.19	1.05	0.94	0.67
50 in.	θ	38°	48°	53°	57°	60°	64°	66°	69°	70°	75°
1270 mm	β	3.90	2.39	1.82	1.50	1.28	1.01	0.84	0.72	0.63	0.41
100 in.	θ	42°	56°	62°	66°	69°	73°	75°	77°	78°	81°
2540 mm	β	3.55	1.87	1.35	1.06	0.88	0.65	0.52	0.43	0.37	0.23
200 in.	θ	46°	64°	71°	74°	77°	80°	82°	83°	84°	85°
5080 mm	β	3.19	1.39	0.90	0.66	0.53	0.37	0.29	0.23	0.20	0.12

*For β values in MPa units, divide the values in the table by 12.

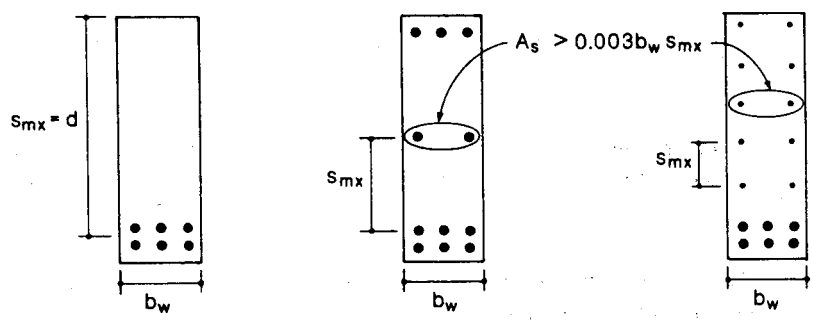

Figure 7-46 Values of crack spacing parameter, s_{mx}.

It is interesting to note that the beams described in Fig. 7-47 contained about the same percentage of longitudinal reinforcement as the roof beams of the Air Force warehouse described in Fig. 7-18. The warehouse beams had an effective depth of about 34 in. (850 mm) and failed at a shear stress of about $1.2\sqrt{f'_c}$ ($0.10\sqrt{f'_c}$ MPa). This shear stress level is consistent with the failure stresses observed for beams about 3 ft (1000 mm) deep in the tests of Shioya et al. Thus it seems likely that the size effect in shear played an important role in the Air Force warehouse collapse.

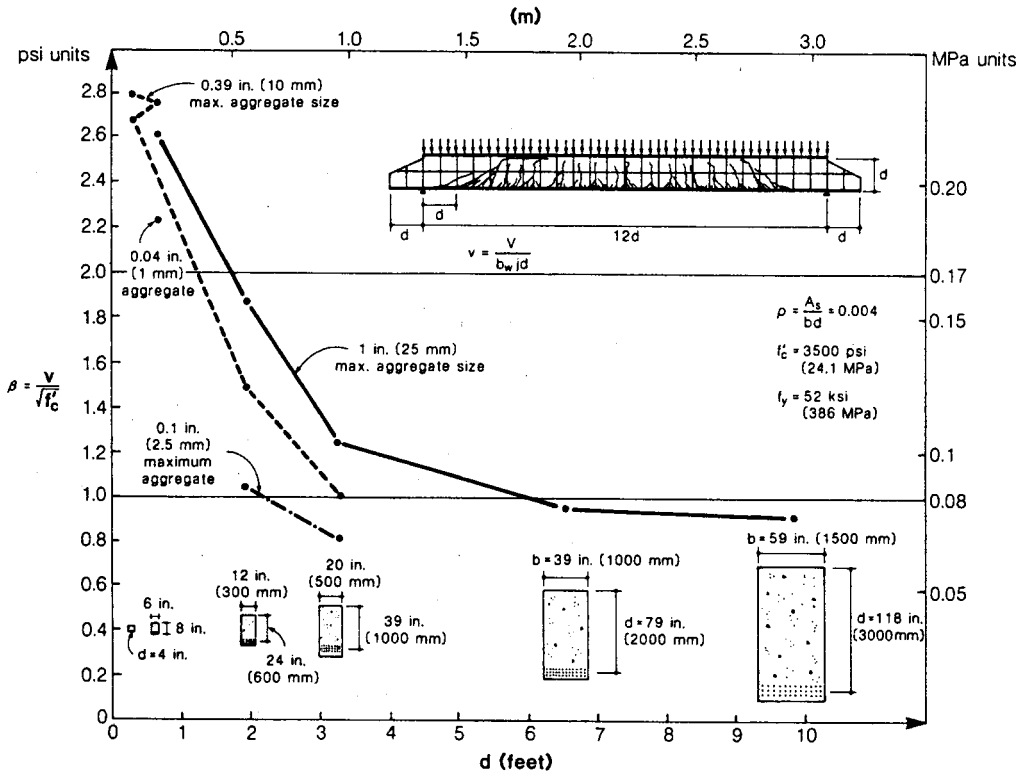

Figure 7-47 Shear stress at failure, on section at distance d from support for series of beams with different depths and different aggregate sizes. Results from Shioya (Ref. 7-41).

The β values in Table 7-4 were derived for a maximum aggregate size of 0.75 in. (19 mm). However, the tabulated values can be used for other aggregate sizes by the use of an equivalent spacing parameter, s_{mxe}. From Eqs. (7-45) and (7-65) β is a function of the parameter $24\epsilon_1 s_{mx}/(a+0.63)$. Hence the values in the table can be used for aggregate sizes other than 0.75 in. (19 mm) if we use an equivalent spacing parameter of

$$s_{mxe} = s_{mx}\frac{1.38}{a+0.63} \quad \text{in.} \tag{7-67a}$$

$$s_{mxe} = s_{mx}\frac{35}{a+16} \quad \text{mm} \tag{7-67b}$$

Thus the largest beam shown in Fig. 7-47, which had a maximum aggregate size of 1.00 in. (25 mm) and an effective depth of 118 in. (3000 mm) would have an equivalent

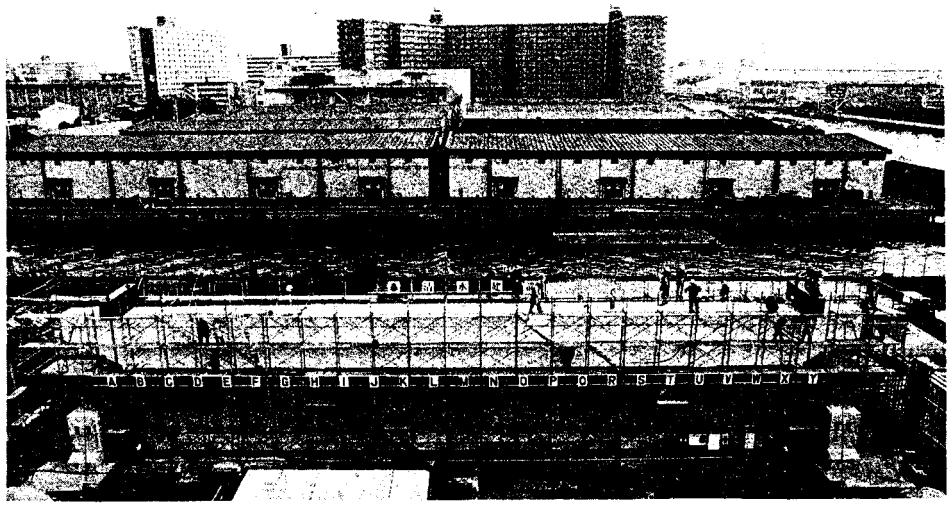

Figure 7-48 Large beam failing in shear. Failure crack between S and X. Photograph courtesy of Shimizu Corporation.

crack spacing of

$$s_{mxe} = 118 \times \frac{1.38}{1.00 + 0.63} = 100 \text{ in. } (2540 \text{ mm})$$

Hence the strength of this large beam could be predicted using the θ and β values given for a crack spacing of 100 in. (2540 mm) in Table 7-4. For example, for ϵ_x equals 0.50×10^{-3}, the θ and β values would be 62° and 1.35. As there is no web reinforcement,

$$\begin{aligned} V = V_c &= \beta\sqrt{f'_c} b_w jd \\ &= \beta\sqrt{3500} \times 59 \times 0.9 \times 118 \\ &= 371\beta = 501 \text{ kips } (2230 \text{ kN}) \end{aligned}$$

If ϵ_x equals 0.50×10^{-3} then, from Eq. (7-53), with A_s equal to 28.3 in^2 (18 240 mm^2)

$$0.50 \times 10^{-3} = \frac{\frac{M}{106} + 0.5 \times 501 \times \cot 62°}{29,000 \times 28.3}$$

Hence M = 29,380 in.-kips = 2450 ft-kips (3320 kNm).

Repeating the calculations above for different values of ϵ_x we obtain the different combinations of shear and moment that are predicted to cause failure. For high values of ϵ_x, yielding of the longitudinal reinforcement will govern the failure and hence the moment values will be found from Eq. (7-62). The predicted shear-moment interaction diagram is shown in Fig. 7-49.

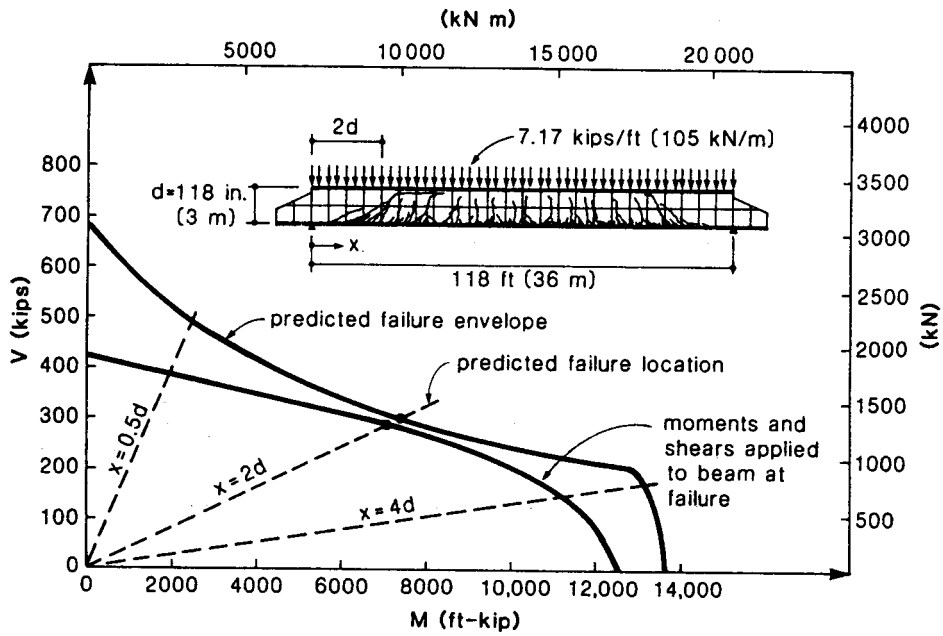

Figure 7-49 Shear-moment interaction diagram showing predicted failure location.

When a uniformly distributed load is applied to a simply supported beam, different sections along the span are subjected to different combinations of shear and moment. Thus the section at the support has the highest shear but no moment, while the section at midspan has the highest moment but no shear. For the large beam reported by Shioya et al. (Ref. 7-40), Fig. 7-49 shows both the predicted failure envelope and the moments and shears applied to different sections of the beam at failure. It can be seen that if the loads were increased by about 4% the loading envelope would touch the failure envelope at a point corresponding to a location in the span which is $2d$ from the support. In the experiment, the failure crack extended from a location about d from the support to a location about $3d$ from the support. Thus, in the experiment, failure occurred at about the location predicted, and at a load that was 96% of the predicted failure load.

7.13 DESIGN EXAMPLE USING MODIFIED COMPRESSION FIELD THEORY

As an example of the use of the modified compression field theory (MCFT), we will redesign the PCI standard single tee described in Sections 7.3 and 7.7.

Step 1: Choose the sections where stirrups will be designed.

The modified compression field theory can be used to calculate the required stirrups at a particular section, given the shear and moment acting at that section. However, a shear failure caused by yielding of the stirrups involves yielding this reinforcement over a length of beam of about $jd\cot\theta$ (see Figs. 7-37 and 7-24). Hence a calculation for one section can be taken as representing a length of beam $jd\cot\theta$ long, with the calculated section being in the middle of this length. Thus, the first section we will check is $0.5jd\cot\theta$ from the face of the support. Additional sections will then be checked at about every $jd\cot\theta$ along the length of the beam.

For the purpose of choosing the design sections, we need to make a conservative estimate of θ (that is, a high value). For this prestressed beam, ϵ_x will probably be close to zero near the support. From Table 7-3 choose θ equal to 30°. Thus $jd\cot\theta$ will equal $0.72 \times 36 \times \cot 30° = 45$ in. = 3.75 ft (1140 mm). Thus the first section we will check will be 22.5 in. (572 mm) from the face of the support. That is, $(22.5 + 4)/12 = 2.21$ ft (673 mm) from the center of the support.

The sections we will check are summarized in Table 7-5. Also given in this table are the factored shear forces, V_u, and the factored moments, M_u, at these sections.

Table 7-5 Design of single tee by modified compression field method.

No.	x ft m	V_u kips kN	M_u ft-kips kN	$d-\frac{a}{2}$ in. mm	jd in. mm	$\frac{v}{f'_c}$	θ deg.	ϵ_x $\times 10^3$	β psi MPa	V_c kips kN	s in. mm	f^*_{ps} ksi MPa
1	2.21 0.67	69.2 308	159 216	23.9 607	25.9 658	0.072	28	0	4.86 0.405	71.2 317	198 5025	111 764
2	5.96 1.82	59.9 266	401 544	25.1 638	25.9 658	0.061	28	0	4.86 0.405	71.2 317	∞	167 1154
3	9.71 2.96	50.5 225	608 824	26.2 665	26.2 665	0.050	36	0.63	2.62 0.218	38.8 173	34.9 886	200 1382
4	13.46 4.10	41.2 183	780 1058	27.3 693	27.3 693	0.038	43	1.61	1.72 0.143	26.6 118	25.9 658	227 1565
5	17.21 5.24	31.8 141	917 1243	28.4 721	28.4 721	0.027	45	2.34	1.54 0.128	24.7 110	63.9 1622	247 1702
6	20.96 6.39	22.5 100	1019 1382	29.6 752	29.6 752	0.017	46	2.72	1.39 0.116	23.3 104	∞	256 1766
7	24.71 7.53	13.2 59	1086 1472	30.7 780	30.7 780	0.007	46	2.85	1.39 0.116	24.1 107	∞	257 1772
8	28.46 8.67	3.8 17	1118 1516	31.8 808	31.8 808	0	46	2.72	1.39 0.116	25.0 111	∞	255 1758
9	30.00 9.14	0	1121 1520	32.3 820	32.3 820	0	46	2.58	1.39 0.116	25.4 113	∞	252 1738

*Stress required in strands.

Step 2: Determine values of $(d - \frac{a}{2})$ and jd.

In this beam the distance from the extreme compression fiber to the centroid of the prestressed reinforcement varies along the length as shown in Fig. 7-10.

The effective shear depth, jd, can be taken as the flexural lever arm, $d - \frac{a}{2}$, but need not be taken as less than $0.9d$ nor $0.72h$. A conservative estimate of the depth of compression, a, can be obtained by assuming that the strands are stressed to their ultimate stress of 270 ksi (1860 MPa). Thus

$$a = \frac{12 \times 0.153 \times 270}{0.85 \times 5 \times 120} = 0.97 \text{ in. (25 mm)}$$

The values of the flexural lever arm, $(d - \frac{a}{2})$, calculated using this value of a are listed in Table 7-5. Also given are the values of jd.

Step 3: Design the stirrups.

For the first section,

$$\frac{v}{f'_c} = \frac{V_u/0.85 - V_p}{b_w j d f'_c}$$
$$= \frac{69.2/0.85 - 6.96}{8 \times 25.9 \times 5}$$
$$= 0.072$$

From Table 7-3, and assuming that ϵ_x is zero, choose θ equal to 28°. While interpolation could be used when choosing values from Table 7-3, it is more convenient to take the value from the next higher row and the next higher column.

From Eq. (7-53),

$$\epsilon_x = \frac{159 \times 12/25.9 + 0.5 \times 69.2 \cot 28° - 12 \times 0.153 \times 152}{29,000 \times 12 \times 0.153}$$
$$= -2.64 \times 10^{-3}$$

Because Eq. (7-53) neglects the stiffness of the concrete it will overestimate compressive strains. Hence ϵ_x will actually be between zero and -2.64×10^{-3}. Thus we will use the column for ϵ_x equal to zero when using Table 7-3. Hence our choice of θ equal to 28° was appropriate.

From Table 7-3, with ϵ_x equal to zero and v/f'_c equal to 0.075 we find that β equals 4.86. Hence, from Eq. (7-43)

$$V_c = 4.86\sqrt{5000} \times 8 \times 25.9$$
$$= 71.2 \text{ kips (317 kN)}$$

Thus

$$V_s = V_u/\phi - V_c - V_p$$
$$= 69.2/0.85 - 71.2 - 6.96$$
$$= 3.25 \text{ kips (14 kN)}$$

That is, only a small quantity of stirrups is required near the support. We will use #3 double-legged stirrups, with f_y = 60 ksi (414 MPa). Hence, from Eq. (7-52),

$$s \leq \frac{0.22 \times 60 \times 25.9 \cot 28°}{3.25}$$
$$\leq 198 \text{ in. } (5025 \text{ mm})$$

Hence the stirrups at this section will be governed by maximum spacing requirements.

Repeating the calculations above for the other sections, we obtain the required stirrup spacings listed in Table 7-5.

Figure 7-50 illustrates the amount of stirrups required at different locations in the span. It is of interest that no stirrups are required for sections more than about 20 ft (6 m) from the support and that the sections requiring the most stirrups are located about 13 ft (4 m) from the support. These predictions agree very closely with those made by the ACI method (see Fig. 7-21).

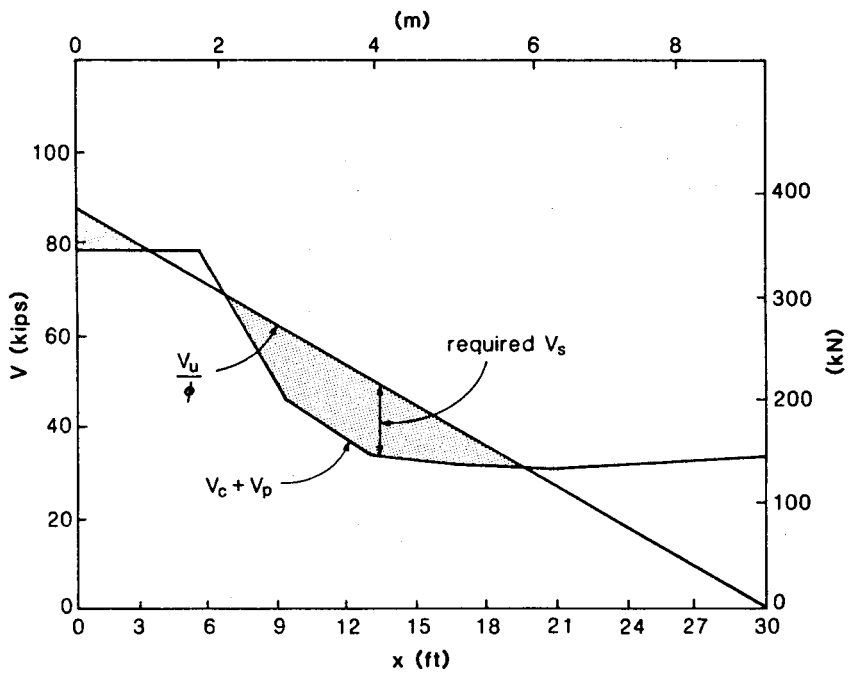

Figure 7-50 Design of stirrups by modified compression field theory.

To satisfy minimum shear reinforcement requirements

$$s \leq \frac{A_v f_y}{50 b_w} = \frac{2 \times 0.11 \times 60,000}{50 \times 8}$$
$$\leq 33 \text{ in. } (838 \text{ mm})$$

To satisfy spacing requirements

$$s \leq 0.75h = 0.75 \times 36$$
$$\leq 27 \text{ in. (686 mm)}$$
$$\text{but } s \leq 24 \text{ in. (610 mm)}$$

Hence a stirrup spacing of 24 in. (610 mm) will satisfy strength, minimum reinforcement, and maximum spacing requirements. Thus the stirrup arrangement shown in Fig. 7-21a will be used.

Step 4: Design the longitudinal reinforcement.

The longitudinal reinforcement must be capable of resisting the moment and the axial tension caused by the shear. The tensile force that will be required in the reinforcement on the flexural tension side of the member is given by Eq. (7-62) as

$$A_{ps}f_{ps} = \frac{M_u}{\phi jd} + \left(\frac{V_u}{\phi} - 0.5V_s - V_p\right)\cot\theta$$

Because we are providing more stirrups than are required, we will determine the actual value of V_s at each section since an increase in V_s will decrease the required force in the longitudinal steel. At the first section, where θ equals 28°,

$$V_s = \frac{0.22 \times 60 \times 25.9 \times \cot 28°}{24}$$
$$= 26.8 \text{ kips (119 kN)}$$

Thus

$$A_{ps}f_{ps} = \frac{159 \times 12/0.9}{23.9} + \left(\frac{69.2}{0.85} - 0.5 \times 26.8 - 6.96\right)\cot 28°$$
$$= 89 + 115 = 204 \text{ kips (905 kN)}$$

Hence the tensile stress required in the strands is

$$f_{ps} = \frac{204}{12 \times 0.153} = 111 \text{ ksi (765 MPa)}$$

Repeating these calculations for the other sections we obtain the required stresses listed in Table 7-5. From these values it can be seen that the longitudinal reinforcement is most highly stressed at section 7.

From Eq. (6-7) we can develop at this location, at least the following stress in the strands:

$$f_{ps} = 270\left(1 - \frac{0.28}{0.80} \cdot \frac{12 \times 0.153 \times 270}{120 \times 31.2 \times 5}\right)$$
$$= 267 \text{ ksi (1844 MPa)}$$

As the strands can provide a stress of 267 ksi (1844 MPa), while the required stress is 259 ksi (1788 MPa), the longitudinal reinforcement in the central region of the beam is adequate.

Figure 7-51 compares the required tensile force in the reinforcement at different locations along the span with the tensile force that can be provided by the pretensioned strands. Note that in the middle third of the beam, the shear causes only a very small increase in longitudinal tension. However, near the support it is the shear that is causing most of the tension in the longitudinal reinforcement. From Fig. 7-51, it can be seen that the strands alone will not be capable of providing all of the tension required at the face of the support. At this location, where the moment is very small, the required tension is

$$T = \left(\frac{V_u}{\phi} - 0.5V_s - V_p\right)\cot\theta \tag{7-68}$$

While Eq. (7-68) was derived from Eq. (7-62) it can also be determined on the basis of the free-body diagram shown in Fig. 7-52 by taking moments about point O. Thus

$$T = \left(\frac{73.9}{0.85} - 0.5 \times 26.8 - 2.23\right)\cot 28°$$
$$= 134.1 \text{ kips } (597 \text{ kN})$$

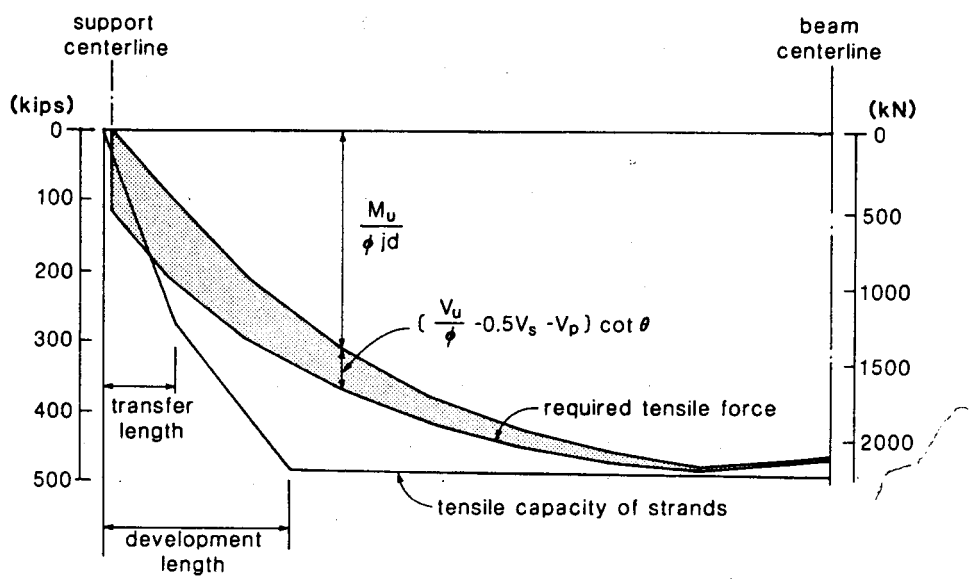

Figure 7-51 Comparison of required tensile force in reinforcement with tensile capacity of strands.

Hence the tensile stress required in the strands at this location is $134.1/(12 \times 0.153) = 73.0$ ksi (503 MPa). As this location is just 8 in. (203 mm) from the free end of the beam (see Fig. 7-9), the tensile stress the strand can resist will be limited by its bond strength. The ACI Code (Ref. 7-2) suggests that the stress in the strand can be assumed to vary linearly from zero at the free end to the effective prestress, f_{se}, over a distance of 50 strand diameters. Hence the stress that the strand can resist at the inner edge of the bearing area is

$$f_{ps} = \frac{8}{50 \times 0.5} \times 152$$
$$= 48.6 \text{ ksi (335 MPa)}$$

Therefore the strands can resist a tensile force of $48.6 \times 12 \times 0.153 = 89.2$ kips (397 kN), which is 44.9 kips (200 kN) less than the required force. If two #6 bars, welded to an embedded anchor plate, are provided at the support, the additional tension that can be resisted will be $2 \times 0.44 \times 60 = 52.8$ kips (235 kN), which will cover the deficiency.

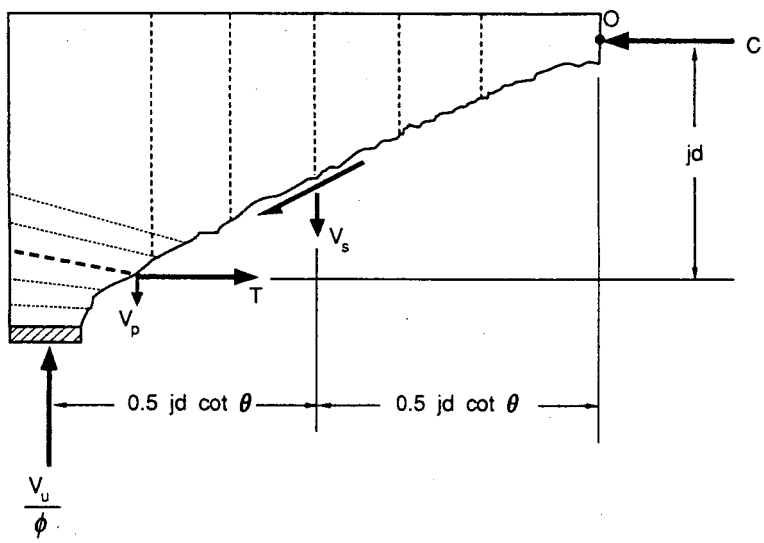

Figure 7-52 Free-body diagram of end region of beam.

It is a serious deficiency of the current ACI shear design provisions that they ignore the fact that shear causes high tension in the longitudinal reinforcement at the face of a support.